

On-device Anomaly Detection in Conveyor Belt Operations

Luciano S. Martinez-Rau, Yuxuan Zhang, *Graduate Student Member, IEEE*, Bengt Oelmann,
and Sebastian Bader, *Senior Member, IEEE*

Abstract—Mining 4.0 leverages advancements in automation, digitalization, and interconnected technologies from Industry 4.0 to address the unique challenges of the mining sector, enhancing efficiency, safety, and sustainability. Conveyor belts are crucial in mining operations by enabling the continuous and efficient movement of bulk materials over long distances, which directly impacts productivity. While detecting anomalies in specific conveyor belt components, such as idlers, pulleys, and belt surfaces, has been widely studied, identifying the root causes of these failures remains critical due to factors like changing production conditions and operator errors. Continuous monitoring of mining conveyor belt work cycles for anomaly detection is still at an early stage and requires robust solutions. This study proposes two distinctive pattern recognition approaches for real-time anomaly detection in the operational cycles of mining conveyor belts, combining feature extraction, threshold-based cycle detection, and tiny machine-learning classification. Both approaches outperformed a state-of-the-art technique on two datasets for duty cycle classification in terms of F1-scores. The first approach, with 97.3% and 80.2% for normal and abnormal cycles, respectively, reaches the highest performance in the first dataset while the second approach excels on the second dataset, scoring 91.3% and 67.9%. Implemented on two low-power microcontrollers, the methods demonstrated efficient, real-time operation with energy consumption of 13.3 and 20.6 μJ during inference. These results offer valuable insights for detecting mechanical failure sources, supporting targeted preventive maintenance, and optimizing production cycles.

Index Terms—Anomaly detection, conveyor belt, edge computing, industry 4.0, low-power microcontroller, machine learning,

tinyML.

I. INTRODUCTION

The advancement in Industry 4.0 has transformed industrial operations, redefining manufacturing and production processes by harnessing the power of automation and digitalization. Industry 4.0 creates a framework where intelligent, connected devices enable data sharing and decision-making across processes, strategically integrating cutting-edge technologies such as the Internet of Things, machine learning (ML), big data analytics, and cyber-physical systems [1]. Within this broader context, Mining 4.0 emerges as a specialized domain tailored to the unique challenges of the mining sector. It leverages advanced technologies to streamline exploration, extraction, processing, and transportation processes [2].

Mining companies also invest in these technologies as part of their commitment to safety, sustainability, and resource efficiency. By reducing their environmental footprint, minimizing energy and water waste, and adopting eco-friendly practices, these companies aim to decrease operational risks, ensure compliance with environmental regulations, and align with global sustainability goals [3].

Mining conveyor belts are vital for transporting materials over long distances and rough terrain. These belts allow for continuous and efficient movement of bulk materials, playing a critical role in optimizing productivity and minimizing downtime [4]. The reliable operation of conveyor belts is

Corresponding author: Luciano S. Martinez-Rau (email: luciano.martinezrau@miun.se).

paramount, as unexpected failures can lead to significant production interruptions, safety risks, and substantial economic losses. Therefore, detecting faults and anomalies in conveyor systems is essential, as it can reduce unexpected downtimes, prevent further damage, and maintain efficient operational workflows [5].

Conveyor belt systems commonly feature various sensors to monitor their operational status and detect early warning signs of mechanical issues. Researchers have developed numerous methodologies using classic ML and deep learning to detect specific faults, such as idler and pulley defects [6], belt damages [7], reduced belt thickness [8], and belt deviation [9]. These approaches leverage data from vibration, thermal, X-ray, acoustic, radio-frequency, and camera sensors to identify these critical anomalies [10]. While considerable attention has been paid to detecting failures in individual components, finding the root causes of failures is of utmost importance. Failures may occur due to changing production conditions, incorrect control settings, operator errors, or equipment malfunctions, emphasizing the need for robust, continuous operation monitoring of conveyor belts [11].

In various industrial applications, such as predictive maintenance, manufacturing, infrastructure, and energy management, time-series data are employed to detect anomalies in operational productive processes using techniques like statistical analysis, data trend evaluation, and process mining [12], [13]. However, many existing methods are computationally intensive or require complex, costly sensor installations, limiting their feasibility in dynamic real-world environments. Due to these constraints, detecting anomalies in the mining sector remains especially challenging.

Regarding continuous monitoring of mining conveyor belts using time-series data, Chiong *et al.* [14] introduced unsupervised clustering models to detect anomalies in the cycle time of pumps responsible for greasing machine parts, while Cheng *et al.* [15] analyzed communication traffic data from a coal mine system to identify operational anomalies and

potential cyberattacks. Anomaly deviations of a short belt were studied in controlled laboratory conditions with inertial measurement units using a small dataset [16]. Recently, Martinez-Rau *et al.* [17] developed a two-stage pattern recognition system for real-time anomaly detection in conveyor belts, using a TinyML classifier to identify internal operational modes [18], followed by pattern-matching rules to classify duty cycles. Although effective in low-power microcontrollers (MCUs), this method relies on accurately classifying internal operation modes and has not been tested for robustness under different environmental conditions. This work is an extension of the former study by presenting two alternative pattern recognition approaches for real-time anomaly detection on low-power MCUs. The first approach uses belt speed to mark the start and end of duty cycles, classifying them through pattern-matching techniques. The second approach employs a TinyML classifier trained to identify anomalous cycles while accounting for possible misclassifications in internal operation modes.

The main contributions are the following: (i) It presents and evaluates two low-computational pattern recognition approaches for identifying abnormal conveyor belt usage in real-time on resource-constrained devices. (ii) The approaches are tested for generalization on an additional dataset. (iii) The approaches are optimized using quantization and implemented on two low-power MCUs, measuring power consumption, memory usage, and inference time.

The structure of the remaining parts of the article is as follows: the operation of the mining conveyor belt is detailed in Section II. Section III describes the data collection, the proposed approaches, the conducted experiments, and the evaluation methodology. Section IV presents the results and their interpretation. Finally, the conclusion and future research lines are discussed in Section V.

II. CONVEYOR BELT OPERATION

A hydraulic conveyor belt system operates by harnessing fluid power to drive the movement of the belt through hydraulic

components. It is a highly efficient continuous transport mechanism, capable of moving heavy loads over long distances. In this system, hydraulic charge pumps pressurize fluid, which is directed through control valves. These valves regulate the flow and direction of oil to drive the hydraulic motors attached to the drive pulleys or rollers of the conveyor belt. The resulting rotational motion propels the belt, facilitating the seamless transportation of materials along the designated path. The control system provides flexibility in adjusting the speed and direction of the belt, offering precise control over its operation. Moreover, sensors connected to the control system continuously allow the tracking and logging of key hydraulic parameters.

The specific conveyor belt used in this study can work in four different operation modes:

- *Off*: the system is not powered.
- *Idle*: the charge pumps are running, but the belt remains stationary.
- *Operational*: the charge pumps and belt are active, but no load is transported.
- *Active*: the charge pumps and belt operate, and the belt is transporting material.

The transitions between these modes can be aggregated to form two distinct types of operational cycles:

- *Normal* operation refers to the typical and expected use of the conveyor system. This cycle begins with a transition from *Idle* to *Operational*, initiated by the operator to start belt movement. When material is loaded onto the belt, the system shifts to *Active* mode. The system remains in this mode while the load is transported. Once the load is cleared, two scenarios can occur: (i) the operator deactivates the belt, returning the system to *Idle* mode, or (ii) the belt continues moving without a load, transitioning from *Active* back to *Operational* until it is turned off and returns to *Idle*. Thus, the full sequence of a normal operation cycle is either *Idle-Operational-Active-Operational-Idle* or *Idle-Operational-Active-Idle*.

- *Abnormal* operation involves deviations from normal usage patterns, leading to energy waste and excessive wear on mechanical components. These cycles begin with a transition from a static belt position (*Off* or *Idle*) to a moving position (*Operational* or *Active*), followed by a return to a static position. Any sequence that differs from a normal cycle is classified as abnormal. For instance, the sequence *Idle-Operational-Idle* is considered abnormal because the belt moves but does not transport any load. Another example of an abnormal cycle is *Idle-Operational-Active-Operational-Active-Operational-Idle*, which indicates that the load was not transported continuously, but in two portions, leading to inefficient operation.

III. MATERIALS AND METHODS

A. Datasets

This study utilized two datasets, each derived from parameters monitored by the control system of a conveyor belt located in Kiruna, Sweden. An incremental encoder with a pulsed output was employed to measure the number of motor revolutions per minute (rpm). Additionally, pressure sensors recorded both the high- and low-pressure of the hydraulic motor. These sensors were integrated into the control system through a 4-20 mA interface. The collected sensor data underwent preprocessing to provide a sampling rate of one measurement per minute retrieved from the control system's user interface. For each sensor, the one-minute interval values represent the average of all readings collected at the sensor's nominal sampling frequency.

The first dataset, namely DS1, comprises data from the entire months of June 2021, October 2021, January 2022, and April 2022, each representing one of the four seasons. This temporal coverage allowed for a broad range of external temperatures, ranging from -26.1 to 26.0 °C, significantly impacting oil viscosity in the conveyor system and, consequently, the observed pressure levels. The second dataset, namely

DS2, was collected from the same conveyor belt during the whole months of June, August, Oktober, and December 2023 with external temperature between -29.0 to 26.0 °C. Figure 1 compares DS1 and DS2, showing similar high-pressure and speed values distributions. Low-pressure values of DS2 are different than in DS1 covering a bigger value range with noteworthy differences in the quartiles. This difference could be caused by machine wear and maintenance.

DS1 contains approximately 170,000 one-minute state samples, labeled according to operational states: 10,566 samples (6.2%) correspond to the *Off* state, 123,225 (72.7%) to the *Idle* state, 11,454 (6.8%) to the *Operational* state, and 24,299 (14.3%) to the *Active* state. Additionally, 603 duty cycles were labeled, with 496 cycles (82.3%) categorized as normal and 107 cycles (17.7%) as abnormal. DS2 contains 751 and 194 normal and abnormal duty cycles. DS1 was used to develop and evaluate the proposed approaches, while DS2 was used to assess the generalization and robustness of the approaches in a different dataset.

The start and end timestamps, along with the ground truth labels for the operation modes and duty cycles, were determined by analyzing the waveform patterns using the Imagimob Studio software (Imagimob AB, Stockholm, Sweden) in collaboration with hydraulic system experts.

B. Algorithms

This study explores a state-of-the-art and two novel approaches to identify anomalies in conveyor belt operations. The approaches classify the duty cycle usages of a conveyor belt applying pattern recognition techniques.

- 1) *Approach-1* proposed by Martinez-Rau *et al.* [17], consists of four consecutive stages (Fig. 2a) and serves as a baseline. The algorithm takes as input the three 1-min sensed variables (motor shaft rotational speed, and the high- and low-pressure of the hydraulic motor), which are used to extract a set of 12 features. Four features consist of the three input values and the differential

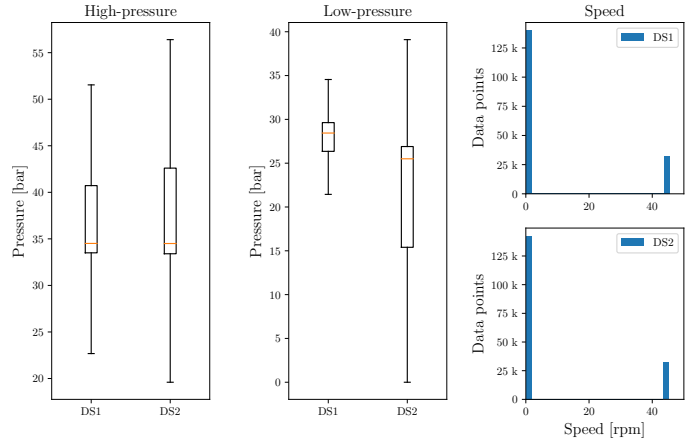


Fig. 1: Box plots and histograms of the sensed input variables in DS1 and DS2.

pressure between the high- and low-pressure. The other eight features are the former four features' third- and fifth-order moving averages, effectively capturing fast and slow variations in the input variables. The complete feature set feeds an ML model to classify the operation modes labeled every 1 min. Since variations in the operation modes typically occur at lower frequencies, a third-order median filter smooths the predicted labels to reduce label fragmentation. Finally, transitions in the filtered state labels are analyzed through pattern matching to detect and classify normal and abnormal duty cycles.

- 2) *Approach-2* offers an alternative method for detecting duty cycles (Fig. 2b). Unlike *Approach-1*, which relies on accurately classifying the operation mode labels to detect and classify duty cycles, *Approach-2* bypasses the state classification step and focuses directly on the input speed values. As shown by the histogram in Fig. 1, the speed values tend to cluster around 0 and 45 rpm. Based on this distribution, an empirical threshold of 5 rpm is chosen to determine the boundaries of the duty cycles. Once these boundaries are identified, the remaining steps in *Approach-2* follow a similar process to those in *Approach-1*.

3) *Approach-3* builds on the concept of *Approach-2* but introduces an ML model to classify duty cycles instead of relying on the pattern-matching rules used in the previous approaches (Fig. 2c). By employing an ML-based classifier, *Approach-3* offers the advantage of generating smoother decision boundaries, which can help mitigate the impact of potential misclassifications of the operation modes.

The operation mode and the duty-cycle classifiers are evaluated with different supervised ML algorithms: decision tree (DT), random forest (RF), extra trees (ET) [19], extreme gradient boosting (XGB) [20], Gaussian naive Bayes (NB), and multi-layer perceptron (MLP) neural network [21].

C. Experimental Setup

The experiments were implemented in Python 3.8.10, utilizing the sklearn 1.2.2 package for tree-based and NB algorithms, and TensorFlow 2.13.0 for the MLP. A grid search was performed for hyperparameter tuning to optimize model performance during training. The maximum depth of the DT was set with a restriction of 10, 20, 30, 40, and 50 splits, as well as without restriction. In all cases, the Gini impurity and the Shannon entropy were considered as criteria for the quality split [21]. For the tree-based ensemble algorithms, the number of trees was set to 10, 25, and 50, with maximum tree depths of 4, 6, 8, and 10. The MLP architecture employed a single hidden layer, with the number of neurons varying between 4 and 15. Training was conducted using stochastic gradient descent, with learning rates of 0.1, 0.01, and 0.001.

The proposed three approaches for classifying duty cycles were trained and evaluated in the first experiment using DS1. The operation mode classifiers were trained and tested using a leave-one-month-out cross-validation strategy. In each iteration, three months of data were used for training and hyperparameter optimization, while the remaining month served for testing. To address the class imbalance, synthetic oversampling, and random undersampling techniques were

applied to the minority and majority operation mode classes before training [24].

In *Approach-1* and *Approach-2*, the predicted operation mode labels were used to detect and classify duty cycles based on heuristic rules. Similar to the operation mode classifier, the duty cycle classifier in *Approach-3* was trained and evaluated using leave-one-month-out cross-validation with balanced training data and hyperparameter optimization. The operation mode classifier was trained first, then the duty cycle classifier was trained and evaluated using the predicted operation mode labels across the four months. This approach allows the duty cycle classifier to learn and adapt to potential misclassifications made by the operation mode classifier.

The generalization capabilities of the proposed approaches were evaluated in the second experiment, where the operation mode and duty cycle classifiers were trained on the entire DS1 dataset and tested on DS2. During training, hyperparameter optimization and class balancing techniques were applied, as in the first experiment.

A key factor to consider was the real-time operational requirements for anomaly monitoring in conveyor belts. To assess resource-constrained hardware requirements, the best-performing models in each dataset were implemented in C code. The best-performing ML models from the previous two experiments were converted to C code using the emlearn 0.19.3 package¹ for tree-based and NB models, and LiteRT² for the MLP. Similar to the second experiment, the models were trained on DS1 and tested on DS2. The energy consumption, memory usage, and algorithm performance were analyzed using ML models with 32-bit float resolutions and post-training 8-bit integer full model quantization. The compiled C code, using arm-none-eabi-g++, was deployed on two MCU boards: the Raspberry Pi Pico and the Arduino Nano Sense 33 BLE Lite. Table I provides the specifications of these boards.

¹<https://github.com/emlearn/emlearn/tree/0.19.3>

²<https://ai.google.dev/edge/litert>

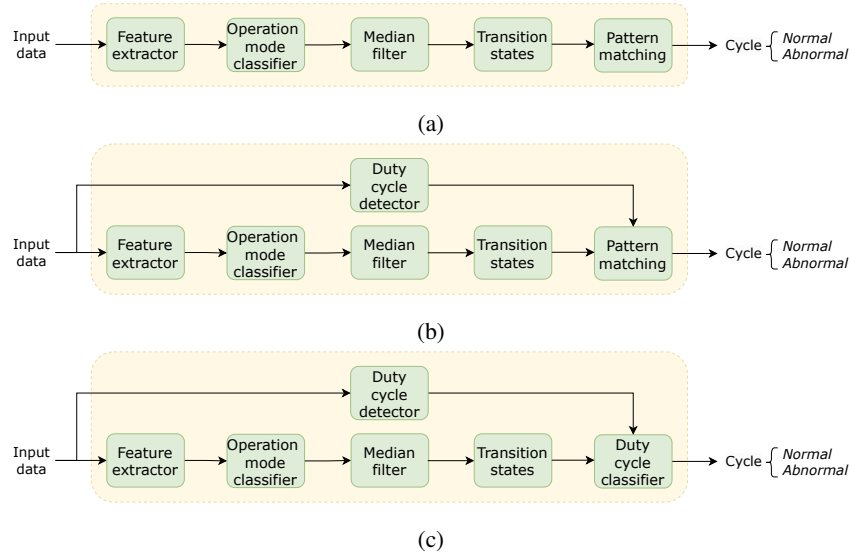


Fig. 2: Flow diagram of the proposed approaches: (a) *Approach-1*, (b) *Approach-2*, and (c) *Approach-3*.

TABLE I: Main properties of the MCU platforms

MCU	CPU core	Test Board	CPU frequency	SRAM	Flash	FPU	Current consumption	Voltage
nRF52840 [22]	ARM Cortex M4	Arduino Nano BLE Sense 33 Lite	64 MHz	256 kB	1 MB	✓	52 μ A/MHz	3.3 V
RP2040 [23]	Dual-core ARM Cortex M0+	Raspberry Pi Pico	133 MHz	256 kB	2 MB	×	75 μ A/MHz	3.3 V

The temporal alignment between the reference and recognized duty cycles has to be considered to evaluate duty cycle classification performance. The assessment was carried out using the `sed_eval` package [25], which applies three criteria for correct duty cycle recognition: (i) the class of the classified cycle must match the reference cycle, (ii) the start timestamp must lie within the reference onset \pm a predefined tolerance, and (iii) the end timestamp must lie within the reference offset \pm a predefined tolerance. A tolerance value of 202.75 seconds was chosen, representing 25% of the minimum duration of a normal duty cycle. A smaller tolerance enforces stricter alignment, while a larger tolerance allows for greater overlap between the reference and recognized labels.

Performance was measured using the F1-score for each class i of duty cycles (normal and abnormal), calculated as:

$$F1 - score_i = \frac{2 * TP_i}{2 * TP_i + FP_i + FN_i}$$

where TP_i counts the number of correctly classified instances of class i , FP_i counts the number of recognized instances of class i that do not exist in the ground truth (insertions), and FN_i counts the number of ground truth instances of class i that are not recognized (deletions). An overall micro-average F1-score was also computed to aggregate the total false positives, false negatives, and true positives across both classes [26]. Except for the deployment on MCUs, each train/test experiment was repeated with different random seeds ten times to ensure robustness. For *Approach-3*, 100 iterations were performed by combining the ten repetitions of the duty cycle classifiers with the ten repetitions of the operation mode classifiers. The final metrics reported are the averages over all repetitions.

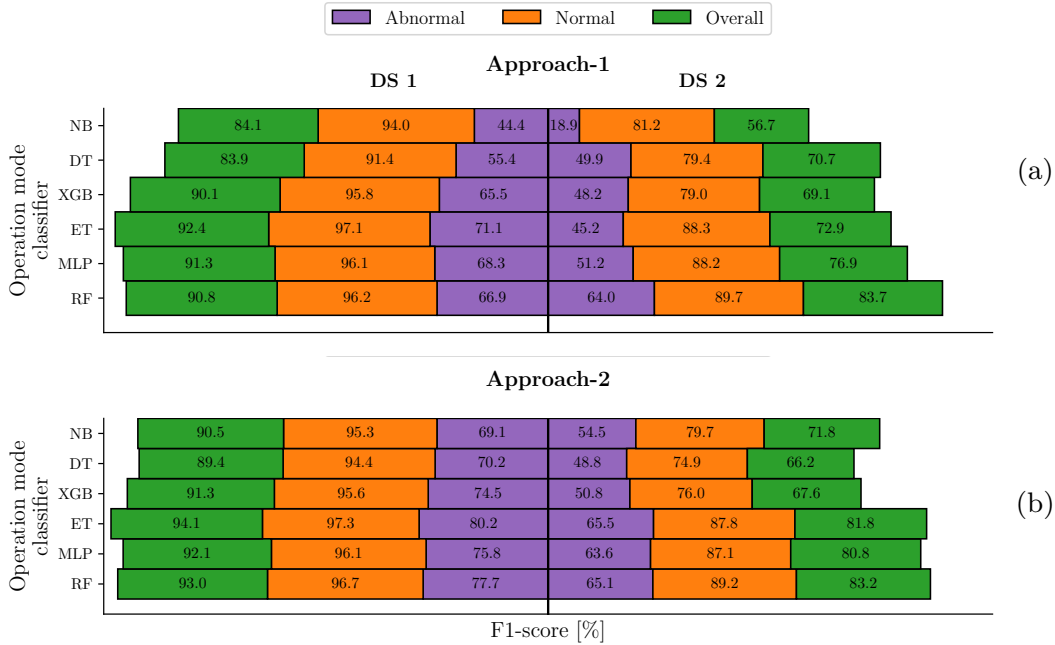


Fig. 3: Diverging bar chart of the accumulative performance of (a) *Approach-1* and (b) *Approach-2*, using different operation mode classifiers in DS1 vs. DS2.

TABLE II: Average F1-score for the duty cycle detection in each dataset. The detection does not depend on the operation mode classifier in *Approach-2* and *Approach-3*.

Approach	Operation mode classifier	DS1	DS2
<i>Approach-1</i>	NB	89.3	61.6
	DT	94.7	97.9
	XGB	94.4	96.4
	ET	95.0	82.4
	MLP	92.5	87.8
	RF	94.2	98.0
<i>Approach-2</i>	-	97.6	99.2
<i>Approach-3</i>	-		

IV. RESULTS AND DISCUSSION

A. Recognition Performance

The detection and classification performance of the approaches using different ML models is presented in terms of F1-scores, averaged over repeated experiments with varying seeds of initialization. Table II shows the detection rates for

operation cycles across approaches. In *Approach-1*, correct cycle detection relies on accurate classification of operation modes, yielding consistent performance above 89.3% across all ML models in DS1. In DS2, the detection performance varies across ML models. While RF, DT, and XGB models show improvement over DS1, MLP, ET, and NB experience declines. In contrast, *Approach-2* and *Approach-3* detect cycles independently of the operation mode classifier, using threshold-based detection (see Fig. 2b and Fig. 2c). This results in 2.5% to 8.2% improvements in DS1 and 1.3% to 37.6% in DS2 over *Approach-1*.

Figures 3 to 5 illustrate the duty cycle classification results for the three approaches in both datasets, revealing significant performance differences. DS1 consistently yields better results than DS2, reflecting the limited generalization capabilities of the approaches and suggesting distinct complexities and class separability challenges between the two datasets. Across all approaches, the abnormal cycle classification is consistently more challenging, with lower F1-scores than those for normal

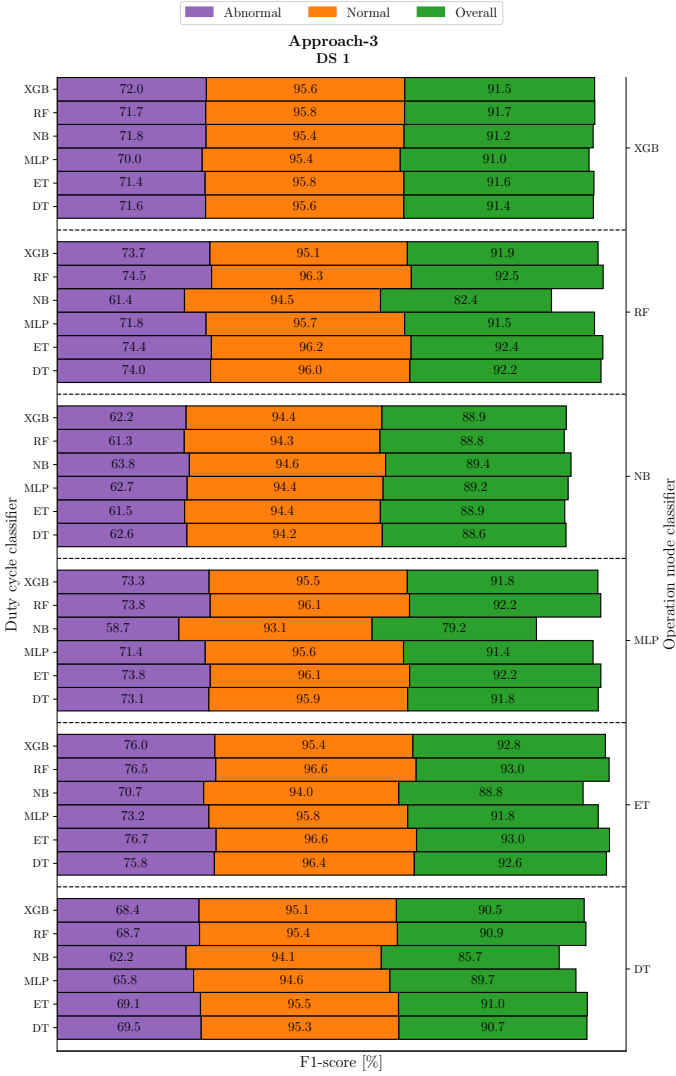


Fig. 4: Grouped bar chart of the accumulative performance of *Approach-3* combining different operation mode and duty-cycle classifiers in DS1.

cycles, due to (i) class imbalance and (ii) the restrictive two possible operation mode sequence combinations in normal cycles compared to the diverse sequences in the abnormal class (see section III-B).

In DS1, *Approach-1* with the ET classifier achieves the highest performance, with an overall F1-score of 92.4%, distinguishing well between normal (97.1%) and abnormal (71.1%) cycles (Fig. 3a). The performance ranking is ET > MLP > RF > XGB > NB > DT, with overall F1-scores decreasing

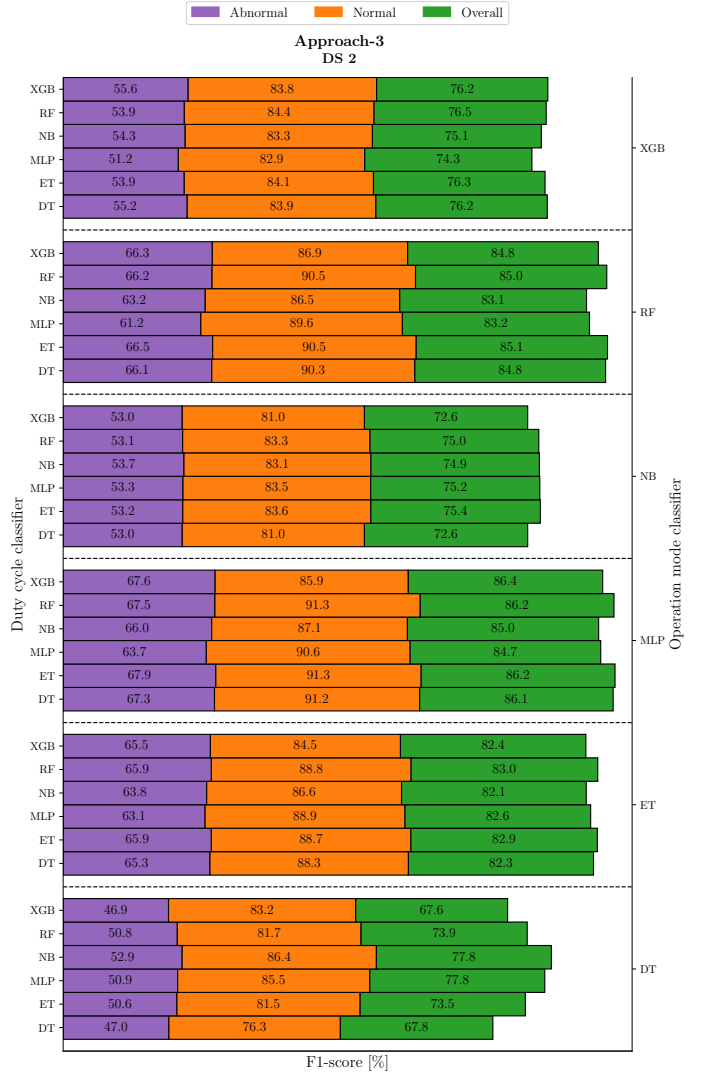


Fig. 5: Grouped bar chart of the accumulative performance of *Approach-3* combining different operation mode and duty-cycle classifiers in DS2.

from 92.4% to 83.9%. In DS2, however, RF outperforms other two models with an overall F1-score of 83.7%, attaining 64.0% for abnormal and 89.7% for normal cycles, suggesting superior generalization. Other models show a decline in abnormal cycle classification performance by 7.2-25.9% and 8.0-16.4% for normal cycles.

Approach-2 demonstrates substantial improvements over *Approach-1* across both datasets (Fig. 3b). In DS1, *Approach-2* maintains a comparable F1-score for normal cycles and shows

TABLE III: Comparison between the selected approaches deployed on the MCUs in terms of classification performance, energy consumption, and memory usage.

Approach	Quantization resolution	F1-score [%]			Arduino Nano BLE Sense 33 Lite			Raspberry Pi Pico		
		Abnormal	Normal	Overall	Energy consumption [μ J/inference]	Flash memory [kB]	RAM [kB]	Energy consumption [μ J/inference]	Flash memory [kB]	RAM [kB]
<i>Approach-2</i> ¹	32-bit float	64.4	87.8	81.4	18.8	265.9	43.1	82.7	209.5	10.4
	8-bit integer	64.9	87.9	81.6	13.7	142.4	43.0	13.3	116.4	10.3
<i>Approach-3</i> ²	32-bit float	65.5	89.2	83.5	26.5	254.9	47.7	40.9	201.3	15.2
	8-bit integer	66.4	89.7	84.1	24.4	242.0	47.4	20.6	191.6	15.0

¹ Using ET as operation mode classifier.

² Using MLP and ET as operation mode and duty cycle classifiers, respectively.

a 7.5-24.6% improvement in abnormal cycle classification. ET again leads with an overall F1-score of 94.0%, achieving 97.3% for normal and 80.2% for abnormal cycles, improving overall performance by 1.7% and abnormal classification by 9.0% over *Approach-1*. In DS2, normal cycle classification with *Approach-2* models is 0.5-4.1% lower than *Approach-1*. However, when using the MLP, ET, or NB models, the abnormal classification improves by 12.4%, 20.2%, and 35.6%, respectively, boosting overall F1-scores by 3.9%, 8.9%, and 15.0%. *Approach-2* with the ET achieves the highest abnormal cycle F1-score, while RF excels in normal cycle and overall F1-scores.

For *Approach-3*, which combines separate classifiers for operation modes and duty cycles, the highest performance in DS1 is using ET for both classifiers, reaching an overall F1-score of 93.0% (96.6% for normal, 76.7% for abnormal) (Fig. 4). However, these results do not surpass the best performance obtained in *Approach-2* using ET. Interestingly, in DS2, the combination of MLP for operation mode and ET for duty cycle classification yields the best performance in *Approach-3*, with an overall F1-score of 86.2% (91.3% for normal, 67.9% for abnormal) (Fig. 5). This result, the highest in DS2 across all approaches, suggests the dual-classifier structure may better address the complexity of DS2. These findings emphasize

the importance of aligning classification methods with dataset characteristics and underscore the potential benefits of sophisticated architectures in complex classification scenarios.

B. MCU Energy Requirements

The best-performing classifier-dependent approaches in each dataset are selected to be deployed in the MCUs using 32-float and 8-integer bit representations. These are *Approach-2* using the ET as operation mode classifier and *Approach-3* using the MLP and ET as operation mode and duty cycle classifiers, respectively. The effect of quantizing to 8-bit does not affect the duty cycle detection, keeping it at 99.2% as in the previous experiments (Table II). The selected models, trained in DS1 and deployed in the MCUs, are evaluated in DS2. The trade-off between classification performance and hardware resource utilization is presented in Table.

The best-performing classifier-dependent approaches for each dataset are selected for deployment on MCUs using either 32-bit float or 8-bit integer representation. These include *Approach-2*, which uses an ET classifier for operation mode classification, and *Approach-3*, which combines an MLP for operation mode classification and ET for duty cycle classification.

Quantizing to 8-bit does not impact duty cycle detection accuracy, which remained at 99.2% as observed in earlier experi-

ments (Table II). Table III illustrates the balance between classification performance in DS2 and hardware resource usage. *Approach-3* achieves superior classification rates for normal, abnormal, and overall classes compared to *Approach-2*, consistent with previous results. Interestingly, both approaches show improved classification performance when quantized to 8-bit, likely due to reduced quantization error. Energy consumption calculations focused on data representing duty cycles, ensuring that all system stages are active (Fig. 2), capturing the peak energy consumption. Reported energy consumption reflects the end-to-end computation for each 1-min input data, averaged across DS2. The time between inputs allows for additional tasks such as MCU peripheral management, conveyor control, or putting the MCU into sleep mode. The Arduino Nano BLE Sense 33 Lite exhibits lower energy consumption for both approaches in the 32-bit float version due to the MCU featuring a floating-point computation unit. In contrast, the Raspberry Pi Pico consumes significantly more power with 32-bit floats but outperforms the Arduino for 8-bit integer representations. Quantizing *Approach-2* reduces program memory usage by 46.4% on the Arduino Nano BLE Sense 33 Lite and 44.4% on the Raspberry Pi Pico, while *Approach-3* presents reductions of 5.1% and 4.8%, respectively. Across both MCUs, 32-bit float and 8-bit integer versions required similar amounts of RAM, as both store data in 32-bit registers.

V. CONCLUSION

This work contributes to Mining 4.0 by proposing two novel approaches for real-time anomaly detection in the continuous operation of hydraulic conveyor belt systems using MCUs. These pattern recognition methods combine feature extraction, threshold-based cycle detection, and TinyML classifiers to accurately identify normal and abnormal duty cycles. By evaluating the performance of different approaches and ML classifiers across two distinct datasets, we identified the most effective methods for achieving accurate and generalizable classification, essential for conveyor belt system monitoring

and predictive maintenance. The first approach achieved higher performance when trained and tested on the same dataset, with an F1-score of 97.3% for normal and 80.2% for abnormal cycles, while the second approach showed superior performance on an independent dataset, achieving 91.3% for normal and 67.9% for abnormal cycles. This comparison highlights both the strengths and adaptability challenges of the methods across varying operational contexts. Furthermore, both approaches outperformed the state-of-the-art method on both datasets, validating their suitability for real-world scenarios.

When deployed in two resource-constrained MCUs, the methods demonstrated stable performance with 32-bit float representation and even slight improvements with 8-bit integer quantization, resulting from minimal quantization error. Energy consumption remained low, at 13.3 μJ and 20.6 μJ per inference on a Raspberry Pi Pico, enabling seamless integration into conveyor control systems and potential for automated preventive actions.

Taking advantage of the fact that the deployed approaches in MCUs use a small amount of the available resources, future work will aim to improve abnormal cycle classification by employing more complex models, such as recurrent neural networks or transformer-based models, to better capture temporal dependencies. Another research direction involves addressing the limited availability of abnormal cycle data through few-shot learning, as well as adding new unlabelled data into the model development using unsupervised ML techniques, which may enhance anomaly detection without extensive labeled datasets.

ACKNOWLEDGMENT

This research was financially supported by the Knowledge Foundation under grant NIIT 20180170.

REFERENCES

- [1] M. S. Rahman, T. Ghosh, N. F. Aurna, M. S. Kaiser, M. Anannya, and A. S. Hosen, "Machine learning and internet of things in industry 4.0: A review," *Meas.: Sens.*, vol. 28, p. 100822, 2023.
- [2] O. Zhironkina and S. Zhironkin, "Technological and intellectual transition to mining 4.0: A review," *Energies*, vol. 16, no. 3, 2023.

- [3] C. Bai, P. Dallasega, G. Orzes, and J. Sarkis, "Industry 4.0 technologies assessment: A sustainability perspective," *Int. J. Prod. Econ.*, vol. 229, p. 107776, 2020.
- [4] M. Andrejiova, A. Grincova, and D. Marasova, "Measurement and simulation of impact wear damage to industrial conveyor belts," *Wear*, vol. 368-369, pp. 400-407, 2016.
- [5] L. Jurdziaik, R. Blazej, and M. Bajda, "Conveyor belt 4.0," in *Proc. Intell. Syst. Prod. Eng. Maint.*, A. Burduk, E. Chlebus, T. Nowakowski, and A. Tubis, Eds. Cham: Springer International Publishing, 2019, pp. 645-654.
- [6] R. L. de Moura, D. Bibancos, L. P. Barreto, A. C. Fracaroli, and E. Martinelli, "Study case in mining industry: Monitoring rollers using embedded lorawan," in *Proc. IEEE Int. Instrum. Meas. Technol. Conf. (I2MTC)*, 2021, pp. 1-5.
- [7] O. Salim, S. Dey, H. Masoumi, and N. C. Karmakar, "Crack monitoring system for soft rock mining conveyor belt using uhf rfid sensors," *IEEE Trans. Instrum. Meas.*, vol. 70, pp. 1-12, 2021.
- [8] A. Kirjanów-Błażej, L. Jurdziaik, R. Błażej, and A. Rzeszowska, "Calibration procedure for ultrasonic sensors for precise thickness measurement," *Meas.*, vol. 214, p. 112744, 2023.
- [9] M. Zhang, K. Jiang, Y. Cao, M. Li, N. Hao, and Y. Zhang, "A deep learning-based method for deviation status detection in intelligent conveyor belt system," *J. Clean. Prod.*, vol. 363, p. 132575, 2022.
- [10] M. Zhang, K. Jiang, Y. Cao, M. Li, Q. Wang, D. Li, and Y. Zhang, "A new paradigm for intelligent status detection of belt conveyors based on deep learning," *Meas.*, vol. 213, p. 112735, 2023.
- [11] Y. Hu, Y. Yan, L. Wang, X. Qian, and X. Wang, "Simultaneous measurement of belt speed and vibration through electrostatic sensing and data fusion," *IEEE Trans. Instrum. Meas.*, vol. 65, no. 5, pp. 1130-1138, 2016.
- [12] Y. Shi, N. Zhang, X. Song, H. Li, and Q. Zhu, "Novel approach for industrial process anomaly detection based on process mining," *J. Process Control*, vol. 136, p. 103165, 2024.
- [13] P. Yan, A. Abdulkadir, P.-P. Luley, M. Rosenthal, G. A. Schatte, B. F. Grewe, and T. Stadelmann, "A comprehensive survey of deep transfer learning for anomaly detection in industrial time series: Methods, applications, and directions," *IEEE Access*, vol. 12, pp. 3768-3789, 2024.
- [14] R. Chiong, Z. Hu, Z. Fan, Y. Lin, S. Chalup, and A. Desmet, "A bio-inspired clustering model for anomaly detection in the mining industry," in *Bio-Inspired Computing Models and Algorithms*. World Scientific, 2019, ch. 5, pp. 133-155.
- [15] Z. Cheng, B. Cui, and J. Fu, "Rethinking the operation pattern for anomaly detection in industrial cyber-physical systems," *Appl. Sci.*, vol. 13, no. 5, 2023.
- [16] S. N. Matos, O. F. Coletti, R. Zimmer, F. U. Filho, R. C. L. de Carvalho, V. R. da Silva, J. L. Franco, T. V. B. Pinto, L. G. D. de Barros, C. M. Ranieri, B. E. Lopes, D. F. Silva, J. Ueyama, and G. Pessin, "Machine learning techniques for improving multiclass anomaly detection on conveyor belts," in *Proc. IEEE Int. Instrum. Meas. Technol. Conf. (I2MTC)*, 2024, pp. 1-6.
- [17] L. S. Martinez-Rau, Y. Zhang, B. Oelmann, and S. Bader, "Tinyml anomaly detection for industrial machines with periodic duty cycles," in *Proc. IEEE Sensors Appl. Symp. (SAS)*, July 2024, pp. 1-6.
- [18] L. Capogrosso, F. Cunico, D. S. Cheng, F. Fummi, and M. Cristani, "A machine learning-oriented survey on tiny machine learning," *IEEE Access*, vol. 12, pp. 23 406-23 426, 2024.
- [19] P. Geurts, D. Ernst, and L. Wehenkel, "Extremely randomized trees," *Mach. Learn.*, vol. 63, pp. 3-42, 2006.
- [20] T. Chen and C. Guestrin, "Xgboost: A scalable tree boosting system," in *Proc. 22nd ACM SIGKDD Int. Conf. Knowl. Discov. Data Min.* New York, NY, USA: Association for Computing Machinery, 2016, p. 785-794.
- [21] T. Hastie, R. Tibshirani, J. H. Friedman, and J. H. Friedman, *The elements of statistical learning: data mining, inference, and prediction*. Springer, 2009, vol. 2.
- [22] *nRF52840 Datasheet. Product Specification v1.11*, Nordic semiconductor, 2024.
- [23] *RP2040 Datasheet. A microcontroller by Raspberry Pi*, Raspberry Pi Ltd, 2024.
- [24] H. He, Y. Bai, E. A. Garcia, and S. Li, "Adasyn: Adaptive synthetic sampling approach for imbalanced learning," in *Proc. IEEE Int. Joint Conf. Neural Netw.* IEEE, 2008, pp. 1322-1328.
- [25] A. Mesaros, T. Heittola, T. Virtanen, and M. D. Plumbley, "Sound event detection: A tutorial," *IEEE Signal Process. Mag.*, vol. 38, no. 5, pp. 67-83, 2021.
- [26] M. Sokolova and G. Lapalme, "A systematic analysis of performance measures for classification tasks," *Inf. Process. Manag.*, vol. 45, no. 4, pp. 427-437, 2009.